

RSC Advances



This is an *Accepted Manuscript*, which has been through the Royal Society of Chemistry peer review process and has been accepted for publication.

Accepted Manuscripts are published online shortly after acceptance, before technical editing, formatting and proof reading. Using this free service, authors can make their results available to the community, in citable form, before we publish the edited article. This *Accepted Manuscript* will be replaced by the edited, formatted and paginated article as soon as this is available.

You can find more information about *Accepted Manuscripts* in the [Information for Authors](#).

Please note that technical editing may introduce minor changes to the text and/or graphics, which may alter content. The journal's standard [Terms & Conditions](#) and the [Ethical guidelines](#) still apply. In no event shall the Royal Society of Chemistry be held responsible for any errors or omissions in this *Accepted Manuscript* or any consequences arising from the use of any information it contains.

Cite this: DOI: 10.1039/xxxxxxxxxx

Electronic platform for real-time detection of bovine serum albumin by means of amine-functionalized zinc oxide microwires[†]

Alessandro Sanginario,^{*a} Valentina Cauda,^a Alberto Bonanno,^a Katarzyna Bejtka,^a Stefano Sapienza,^a and Danilo Demarchi^{a,b}Received Date
Accepted Date

DOI: 10.1039/xxxxxxxxxx

www.rsc.org/journalname

We report on the fabrication of a customized electronic platform for biosensing, integrating onto gold microelectrodes a single functionalized microwire as sensing element and including a custom microelectronic chip for signal readout. As a proof-of-concept, the platform was validated for the real-time detection of Bovine Serum Albumin (BSA) binding onto NH₂-functionalized Zinc Oxide (ZnO-NH₂) microwire. The ZnO-NH₂ microwires were deposited between two gold electrodes by means of dielectrophoresis (DEP) technique. A Quasi-Digital Impedance Converter (QDIC) was conceived to constantly and instantaneously readout the ZnO microwire impedance and transfer data to a laptop. Microelectrodes, QDIC, DEP generator and data analysis were integrated in a stacked-card PCB configuration for a better noise reduction and usability. The system was able to distinguish between different BSA concentrations and to give real-time information about the binding process.

1 Introduction

Sensing devices based on nano- and micrometer-scale structures can provide novel tools for the investigation of physical parameters as well as of a broad range of molecules. Research activities were already devoted to produce sensors able to detect extremely small amounts of analytes, which is particularly important in the context of biosensing. In this field, there is a great demand for low concentration detection and high specificity towards the analyte of interest. The ultimate goal of nano- and microscale-based biosensors is to detect any biochemical and biophysical signal associated with a specific disease at the level of a single molecule or cell. This technology can improve conventional medical practices by enabling early diagnosis of chronic debilitating diseases, ultrasensitive detection of pathogens and long-term monitoring of patients using biocompatible integrated medical instrumentation¹. Moreover, the future impact of nano- and micro-biosensor systems will move to point-of-care diagnostics. Indeed, as soon as the nano- and micro-biosensor technology becomes more refined and reliable, it is expected that it will make its way from the lab to the clinic, where future lab-on-a-chip devices incorporating

an array of nano- and micro-biosensors could be used for rapid screening of a wide variety of analytes at low cost, using small amounts of the patient materials and fluids.

Among all possible biomolecules, protein detection is more challenging than nucleic acid detection for two reasons: (i) protein amplification (like PCR for DNA) does not yet exist, thus leading in many cases to very small concentrations to be detected; (ii) protein sensing needs a very controlled environment (e.g., temperature, contaminations, pH) difficult to reproduce, thus a high accuracy measurement system is required to detect low concentrations. To overcome these challenges, the detection of proteins with biosensors can be implemented by detecting directly the bioanalyte as soon as it binds to two electrode surfaces separated by a nanometer-sized distance (i.e., nanogap). In this case, an effective protein detection in nanogap-based² bioelectronic devices strongly depends on the binding process of the biomolecule onto the electrode surface. Actually, the electron transfer between the protein and the electrode is influenced by four parameters: the biomolecule binding process, the material and the surface properties of the electrodes, the interface between the bioanalyte and the metal electrodes, behaving as the inherent barrier for electron transfer. All these factors can modify the orientation of the protein and its distance from the electrode, thus influencing the biosensor answer. However the strong limitation to this detection process is that the nanogap dimensions should match the biomolecule size, which are in most cases of few nanometers, and the biomolecules

^a Center for Space Human Robotics@PoliTo, Istituto Italiano di Tecnologia, Torino, Italy.
E-mail: alessandro.sanginario@iit.it

^b Department of Electronics and Telecommunication, Politecnico di Torino, Torino, Italy

[†] Electronic Supplementary Information (ESI) available: characterization data for electronic system, control experiment and estimation of protein amount procedure.

has to bridge the two facing electrodes to be successfully detected.

Therefore, a more effective alternative method for biomolecules detection is based on indirect measurement which involves the monitoring of the electrical properties of functionalized sensing nano- or micromaterials during the binding of the target biomolecules^{3,4}. Among these materials, zinc oxide (ZnO) has received great attention having several favorable properties including high electron mobility and a wide band gap (3.3 eV), as well as different sensing abilities toward the pH of solutions^{5,6}, gas molecules⁷, ultraviolet (UV) light⁸, and temperature variations⁹. The advantages associated with a large band gap include high breakdown voltages, robust to large electric fields, and high-temperature and high-power operation, which are quite desirable properties in view of the material integration into electronic circuits. In addition, ZnO can be easily synthesized with wet-chemical methods in various morphologies and shapes, obtaining nanoparticles^{10,11}, nano and micro-wires^{11,12}, multipods¹³, nanotubes¹⁴, flower-like particles^{15,16}, and other structures¹⁷. Complementing its unique chemical qualities, ZnO offers significantly lower fabrication costs by wet chemistry methods when compared to other semiconductors used in nanotechnology. The external surface of the ZnO crystalline structure, particularly when synthesized by wet-chemical low temperature processes¹⁸, exposes several hydroxyl groups (-OH), which can be further used to chemically anchor molecules and functional groups. ZnO crystallizes in the anisotropic wurtzite hexagonal phase, which leads to polar crystalline end surfaces. Particularly, the monocrystalline ZnO micro- and nanowires show an intrinsic polarization due to oxygen plane (negatively charged) and zinc plane (positively charged) placed at the edges of the nanostructure¹⁹. This intrinsic dipole allows to easily align the ZnO micro- and nanowires suspended in a liquid medium exploiting the well-known dielectrophoresis (DEP) process^{8,20}. The DEP technique consists in generating a non-uniform electric field \vec{E} between the metal electrodes where the micro- and nanoparticle has to be assembled. Indeed, the non-uniform \vec{E} induces an attractive force to the ZnO microwires, leading them to move towards the electrodes (i.e., where the \vec{E} is higher), and aligns them following the electric field lines. Other semiconductor nano- or microwires are good candidates for such biosensing but not all of them can be eligible for such task like the ZnO material. Titania nanowires, for example, show similar semiconductor and wide band-gap properties but they can not be guided on the electrical contacts with DEP technique losing the advantage of an easy integration. Other types of exotic materials are too difficult or sometimes impossible to chemically functionalize, for further anchoring and detecting biomolecules. On the other hand, silicon nano- and microwires (SiNW) were extensively studied and exploited. Actually there is a large number of papers in the literature reporting on the use of SiNW between two electrodes as chemical and biomolecule sensors^{4,21}.

For these reasons and for the previous mentioned ZnO properties, following the state-of-the art on bio-nanosensors, this paper studies the real-time protein detection based on functionalized ZnO microwires assembled on gold electrode. A custom mi-

croelectronic chip, called Micro-for-Nano (M4N)²², continuously measures ZnO microwires impedance and transfers data to a laptop that plots and stores them for further analysis. The whole system is designed to be easy-to-use and reliable. In fact, an Arduino²³ board is the interface between the laptop and the customized chip while the integration of the electrodes on the same board of the chip assures low noise and precise measurements. The custom microchip also provides the AC signal to enable the DEP for the ZnO microwire integration process. We used this integrated system to for the real time detection of the Bovine Serum Albumin (BSA) protein, a well-known plasma protein able to bind and transport a range of hydrophilic molecules and showing no electro-active role in its action.

2 Indirect measurement of BSA protein concentration

2.1 ZnO synthesis and functionalization

The ZnO microwires were prepared by hydrothermal method according to Refs.^{5,6}. In detail, 1.48 g zinc nitrate hexahydrate $\text{Zn}(\text{NO}_3)_2 \cdot 6\text{H}_2\text{O}$ (5 mmol, Sigma-Aldrich S.r.l. Milan, Italy) in 10 ml bidistilled water (Direct Q, Millipore Co., Billerica, MA, USA) were slowly dropped into solution of 3.35 g potassium hydroxide (60 mmol, Merck KGaA, Darmstadt, Germany) in 10 ml water under vigorous stirring. The obtained solution was then heated at 70 °C for 5 h in a closed Teflon vessel. The formed ZnO microwires were then collected by filtration, washed thoroughly with water until neutral pH was reached, and dried in air at 60 °C.

The chemical functionalization with aminopropyl groups was carried out with 250 mg (3.075 mmol) of ZnO microwire after outgassing them for 2 h in a glass round flask. Then 0.307 mmol of aminopropyltrimethoxysilane (APTMS; 55.04 mg), corresponding to the 10 mol% of the ZnO molar amount, were added together with 10 ml of toluene, and the solution was refluxed for 24 h under nitrogen atmosphere. The functionalized microwires (ZnO-NH₂ microwire) were then washed with toluene to remove the unbound molecules and then dried at 60 °C overnight.

2.2 Reaction mechanism

The EDC/Sulfo-NHS system has probably been the most successful way of creating zero length crosslinks for decades²⁴. Facilitated through a reactive carbodiimide (EDC) and N-hydroxysulfosuccinimide (Sulfo-NHS) as EDC stabilizer, this coupling procedure is a highly efficient choice for crosslinking proteins or immobilizing proteins to a support. 1-ethyl-3-(3-dimethylaminopropyl) carbodiimide hydrochloride (EDC) is the most readily available and commonly used carbodiimide. One of the main advantages of EDC coupling is the room temperature reaction, enabling to operate with all biological molecules, and its water solubility, which allows direct bioconjugation without dissolution in organic solvents. The addition of Sulfo-NHS stabilizes the amine-reactive intermediate by converting it to an amine-reactive NHS ester, thus increasing the efficiency of EDC-mediated coupling reactions. In this work we constantly and instantaneously (in the order of few ms) monitored each needed step for coupling the carboxyl groups of the BSA protein to the

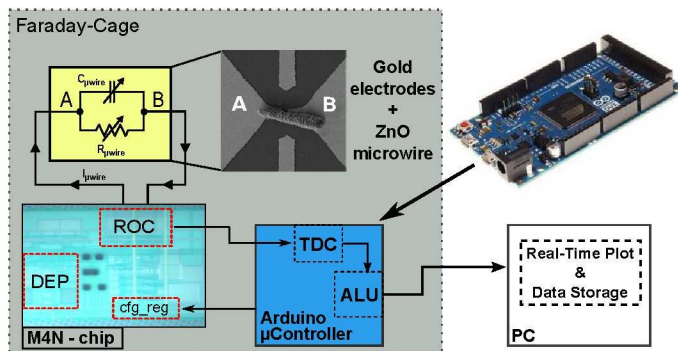


Fig. 1 Block diagram of the electronic acquisition system. M4N chip can apply DEP signal to attract microwire between the two electrodes as shown in the Scanning Electron Microscope image. Such microwire is modeled as a variable RC read by the Read Out Circuit (ROC). Such value is transferred to a microcontroller that elaborates the signal and sends it to a laptop for further analysis. TDC: Time-to-Digital Converter, ALU: Arithmetic Logic Unit, cfg_regs: configuration registers

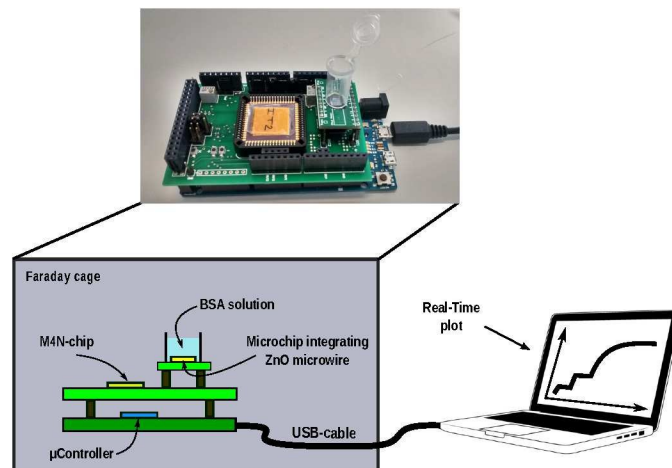


Fig. 2 Picture and schematic drawing of the acquisition system. Arduino board, ROC and sensor chips integrated in a multi-stack PCB and closed in a Faraday cage. Measured data are transmitted to a laptop with a USB cable. Data are then plotted in real-time and stored for further data analysis

amine-functionalized ZnO microwire already deposited on the gold electrodes. In particular we divided the whole EDC amidation process in four steps to clarify the different measured electric impedance outputs:

- measurement of the ZnO-NH₂ microwire-gold junction in air for 30 minutes;
- addition of 250 μ l bi-distilled water and 30 minutes real-time monitoring;
- addition of an equimolar amount of EDC and Sulfo-NHS reagents (5 μ mol) + 125 μ l of bi-distilled water and 30 minutes real-time monitoring;
- injection of 15 or 150 nmol of BSA + 125 μ l of bi-distilled water and monitoring the electric impedance for several hours;

Every solution was prepared few minutes before the addition to the previous step.

The mean value of the current was used as a reference to normalize the measurements, since each microwire has its own impedance value that has to be known for comparing different microwires. All measurements were normalized using the mean value of the measured impedance of each ZnO microwire assembled onto different gold microelectrode. This was needed to compare the results obtained from different ZnO microwires. The selection of this quite long time steps is arbitrarily defined in order to test the stability over time of the proposed whole system. However, the M4N chip constantly measures the microwire impedance with an acquisition time of few milliseconds thus leading to a real-time output.

2.3 Real-time Electronic Acquisition Interface

Considering that the final purpose of this study is the development of an integrated system for the real-time measurement of a protein binding to functionalized ZnO nano- and microwires, we conceived a custom microelectronic chip⁸ able to both apply

a dielectrophoretic signal to attract microwire between two electrodes and read-out the microwire signal (i.e. a current in the pA- μ A range). We integrated the M4N chip on a PCB interfaced with an Arduino board to transfer the measured data to a working station (i.e. a laptop) for data storage and real-time visualization. An Arduino platform was chosen for the large availability of different tools that make easier the development of intuitive user interface, robust data transfer protocol and accessible documentation for future platform improvements. Figure 1 represents the block diagram of the whole system. The current flowing through the ZnO microwire depends on the intrinsic characteristics of the material, here represented by the simple electrical model including the resistance $R_{\mu\text{wire}}$ and the capacitance $C_{\mu\text{wire}}$ in parallel. These electrical parameters are converted by using a Quasi-Digital Impedance Converter (QDIC)⁸ to the digital signal V_{QD} compliant with microcontroller I/Os. The time-to-zero $T_{0,\mu\text{wire}}$ and the time-to-one $T_{1,\mu\text{wire}}$ of the signal V_{QD} carry the sensing information since they are directly proportional to $C_{\mu\text{wire}}$ and $R_{\mu\text{wire}}$. As reported in⁸, the average value of $T_{0,\mu\text{wire}}$ and $T_{1,\mu\text{wire}}$ are accurately calculated in real-time by implementing a Time-to-Digital Converter (TDC) using the internal timers of the microcontroller (μ Controller). $T_{0,\mu\text{wire}}$ and $T_{1,\mu\text{wire}}$ are used in Equations 1 and 2,

$$C_{\mu\text{wire}} = T_{0,\mu\text{wire}} \frac{C_{\text{ref}}}{\Delta T_{0,\mu\text{wire}}} - C_{\text{base}} \quad (1)$$

$$R_{\mu\text{wire}} = a \frac{T_{1,\mu\text{wire}} R_{\text{par}}}{(C_{\text{base}} + C_{\mu\text{wire}}) R_{\text{par}} - a T_{1,\mu\text{wire}}} \quad (2)$$

where a is a constant linked to the design parameter, C_{base} and R_{par} are estimated during calibration step, C_{ref} is an off-chip component, $R_{\mu\text{wire}}$ and $C_{\mu\text{wire}}$ are the calculated electrical properties of the ZnO microwire. The calibration algorithm and these simple equations are also implemented in the microcontroller firmware, so that the device can only transmit the final values to the working station for real-time plot and data storage. Considering that

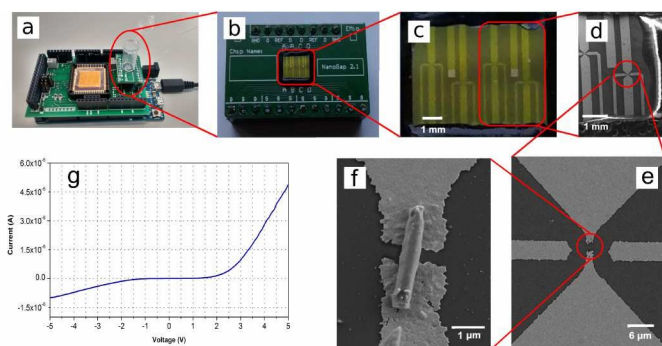


Fig. 3 Complete acquisition system. (a) Electronic control board underneath the sensor board with a polypropylene tube attached to the sensor to keep the chemicals in contact with the sensing element. (b-e) The sensor chip, bonded to a PCB, is composed of four sections of two electrodes plus other two side electrodes (not used in this work). (f) A functionalized ZnO microwire attracted between the two electrodes providing an electrical contact. (g) I-V curve of a ZnO microwire after deposition among the gold electrodes of the microchip.

the creation of chemical links between the BSA proteins and the ZnO microwire involves additional localized charges and the sharing of electrons in the conduction band of ZnO microwire, an increase of $R_{\mu\text{wire}}$ and $C_{\mu\text{wire}}$ is expected during experiments²⁵. The designed QDIC covers a wide range of resistance and capacitance load, which is needed to support large process variations between different microwires. It achieves a measurement accuracy of 1%, and therefore can detect small interactions between the microwire and a low quantity of anchored bio-molecules. Since the measure is represented in the time-domain, the measurement noise of quasi-digital converters corresponds to the jitter of the characteristic oscillation period $T_{\mu\text{wire}} = T_{0,\mu\text{wire}} + T_{1,\mu\text{wire}}$, which can be caused by coupling noise and external interference. In order to detect small quantity of BSA protein and considering that the ZnO microwires are also sensitive to temperature and UV light irradiance variations, a controlled test environment is thus required. Hence, the system has been encapsulated into a bulky Faraday cage with two benefits: a shield for the noise interferences and a repair from ambient light irradiance. Figure 2 shows the experimental setup which includes the developed measurement system and a PC working station for real-time graph visualization. The experiment needs several hours to evaluate the complete binding process between the BSA protein and the ZnO-NH₂ microwire. Hence, the system has been previously evaluated by performing a 24-hours measurement of a known stable impedance in order to identify the presence of output drift of the ROC during measurement. The results (Supporting information Figure S1) have shown stable output with SNR ≥ 44 dB, assuring reliable data during the experiment that involves the ZnO microwire and the BSA protein. The total time duration of the experiment is chemistry-driven since each single measurement can take at most few milliseconds. Thus the system is able to real-time monitor from very fast to really slow reaction kinetics. In the next section the results of preliminary experiment using two different concentrations of BSA protein are presented and discussed in detail.

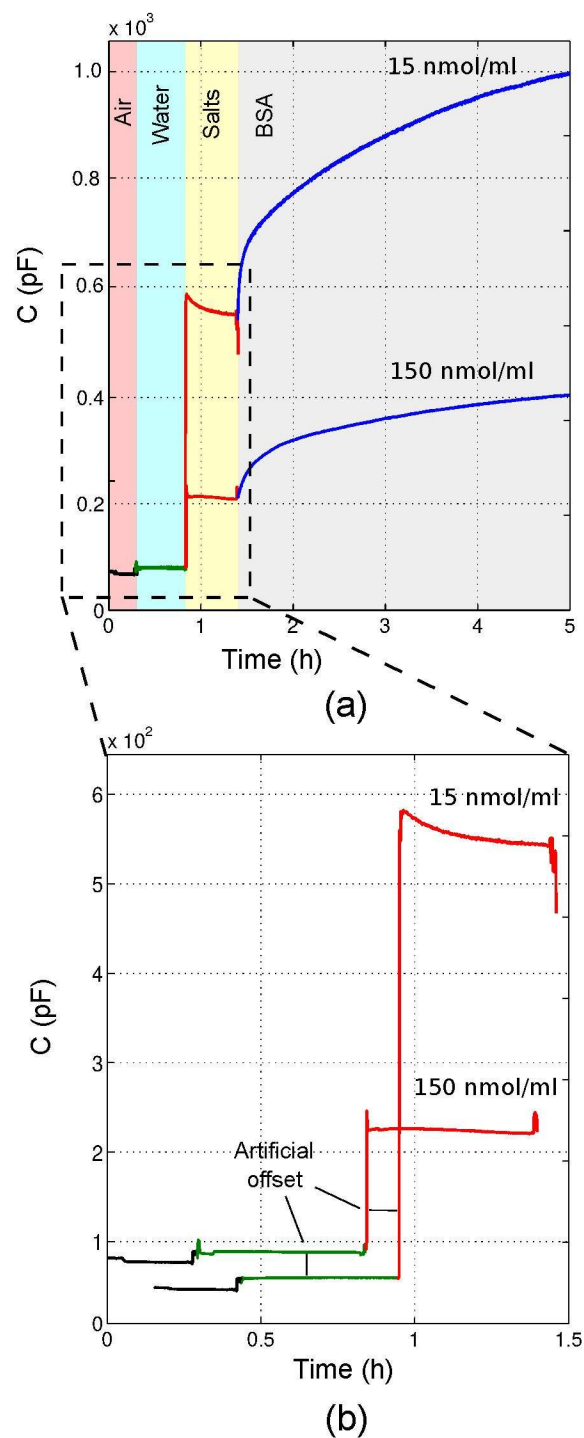


Fig. 4 (a) Real-time measurement of the ZnO-NH₂ capacitance measured during the amidation reaction of the BSA protein continuously observed for five hours. The different reaction steps are highlighted with different colors: ZnO is in air during the first step, then bi-distilled water, EDC and sulfo-NHS reagents, BSA protein (two different concentrations) are added in sequence. (b) Magnification of the first three steps. An artificial offset is added to distinguish the curve trends.

2.4 Experimental setup overview

Figure 3 shows the complete experimental setup. An Arduino board controls the M4N chip described in Section 2.3 mounted

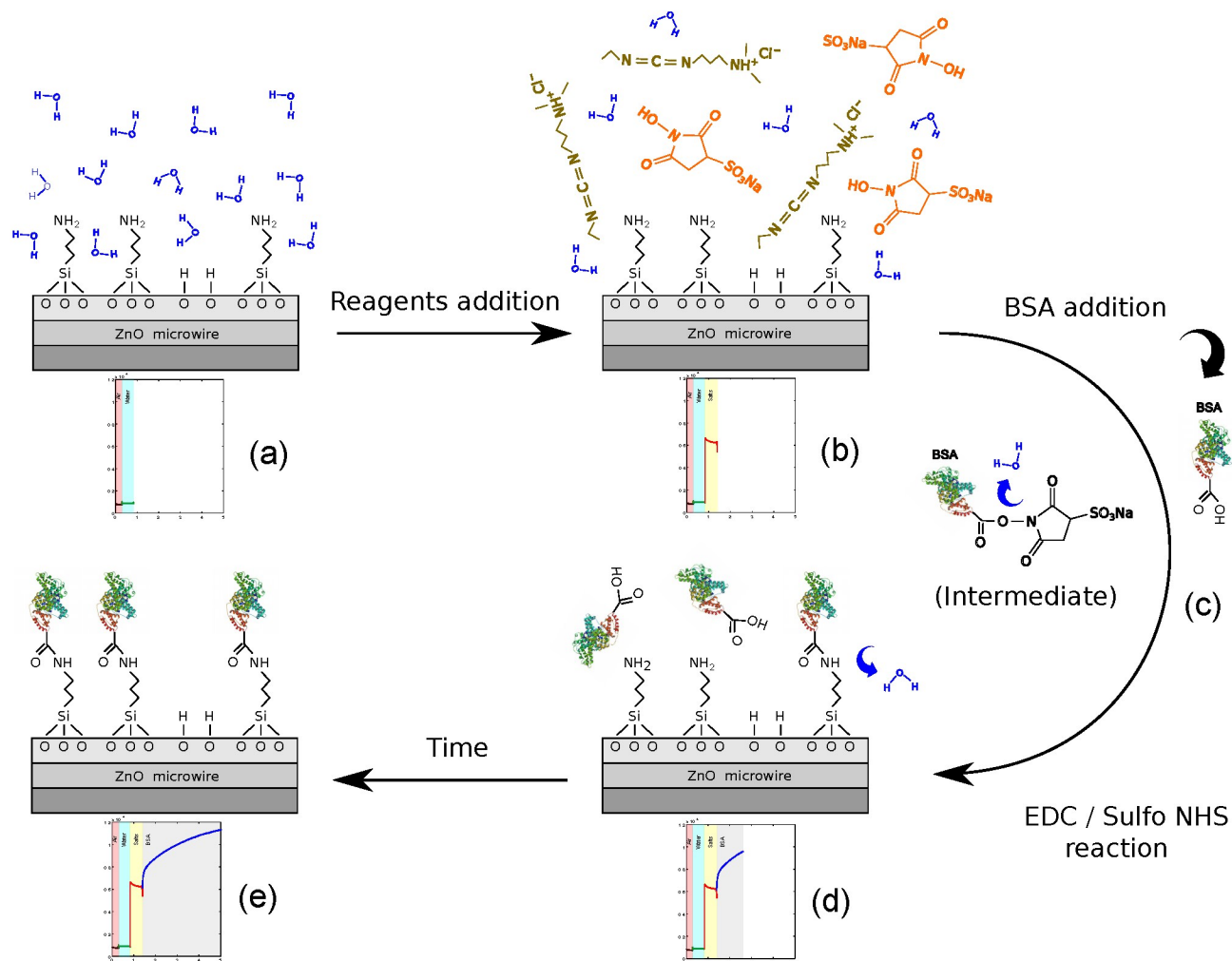


Fig. 5 EDC/Sulfo-NHS/BSA-NH₂ reaction mechanism. (a) Only bi-distilled water does not interact with the ZnO microwire but slightly increases the parallel capacitance at the electrodes (not shown in the picture). (b) EDC and SulfoNHS addition form an electrical double layer on the electrode thus increasing the capacitance. The ZnO microwire is still not affected. (c) BSA addition triggers the EDC/sulfo-NHS reaction creating amine-reactive intermediate compounds. (d) As soon as the intermediate get in contact with ZnO amine groups a reaction occurs linking the BSA carboxyl group to the ZnO amine. The ZnO capacitance start to increase. (e) As long as the crosslinking reaction occurs the capacitance continue to increase until all ZnO reaction sites are saturated.

onto an interface board (Figure 3a). This board also hosts the sensing device composed by four replicas of two facing gold electrodes (thickness 20 nm) deposited by photolithography on a Si wafer with a Ti adhesion layer, as previously reported⁵, with two other side electrodes not used in this work (Figure 3c). A polypropylene plastic tube equipped with a cap was sealed on the sensor chip (Figure 3a) to provide a reservoir for the chemicals and to avoid possible contaminations as one experiment last for several hours. The functionalized ZnO-NH₂ microwires, suspended in isopropanol, were positioned between the sensing electrodes (Figure 3f) by means of DEP technique (3 V_{pp} @ 1 MHz). Once the solvent has completely evaporated, an I-V curve was recorded to check whether the microwire was well positioned or not. A typical ZnO microwire I-V curve (Figure 3g) represents a double Schottky barrier where the threshold voltage changes for every microwire due to many factors such as contact resistance,

microwire characteristics and metal-semiconductor interface. After these integration steps the setup was ready for the proof-of-concept real-time detection experiments, described in the next Section 3.1.

3 Results and discussion

3.1 Real-time electrical monitoring

Figure 4 shows capacitance trends over time for two different BSA concentrations (15 and 150 nmol/ml). Different color segments were used to highlight ZnO-NH₂ continuous measurement during the four experimental steps: (i) ZnO-NH₂ exposed to air (black segment), (ii) bidistilled water addition (green segment), (iii) EDC and Sulfo-NHS reagents addition (red segment) and (iv) BSA addition (blue segment). The behavior of water molecules when in contact with the ZnO-NH₂ surface, as also depicted in Figure 5a, did not show any strong interaction, except the weak hy-

drogen bond formation between hydrogen from the amine group and the oxygen of water. The small capacitance increase, with respect to the previous black segment recorded in air, was due to the different dielectric constant of the water, creating a capacitor in parallel with the ZnO microwire. After about 30 minutes we added EDC and sulfo-NHS reagents needed for the EDC amidation. As expected, they did not react with NH_2 groups present on the ZnO surface (red segments in Figure 4b and scheme of Figure 5b). However, we still recorded a capacitance prompt increase due to the electrical double layer (EDL) formed at the electrodes surface²⁶. Such capacitance change abruptness was no more present when, after about 30 min, BSA protein dissolved in the remaining 50% of water solvent was added. Indeed, following the reaction mechanism already described in Section 2.2, sulfo-NHS, when in contact with carboxyl group of BSA, formed a semi-stable amine-reactive NHS ester (Figure 5c), which then reacted with primary amines, present on the ZnO surface, to form amide crosslinks (Figure 5d,e). Amine reactions took place over a long time period because of many factors including two different reaction kinetics, diffusion coefficients, temperature and pH^{27,28}. Moreover, the higher was the number of the $-\text{NH}_2$ groups already conjugated with the protein, the more difficult was the reaction of other BSA molecules, likely due to steric hindrances of the bulky protein and depletion of reactants with time. Initially, since all $-\text{NH}_2$ sites were free to react, the capacitance of ZnO microwire increased quickly (blue segment in Figure 4 and Figure 5d) in a logarithmic trend up to a plateau due to the complete sites saturation (Figure 5e). Validation of such mechanism interpretation came from the control experiment in which ZnO microwire without NH_2 functionalization was undergone to the same procedure. In this case, air, water, EDC and sulfo-NHS reagents capacitance trends were consistent with the ZnO- NH_2 experiment but after BSA introduction the capacitance remained almost constant (Supporting information Figure S2).

The different capacitances recorded between the two experiments at different concentrations, i.e. 15 and 150 nmol/ml, better evidence the kinetics of the reaction and the related active sites occupation by the BSA bulky molecules. Actually the curve with 15 nmol/ml of BSA in Figure 4a depicts a more gradual increase of the capacitance when the BSA molecules are added, which takes more time to reach the saturation plateau with respect to the experiment having 150 nmol/ml of BSA. In this last case, we attribute the rapid plateau reaching due to the higher concentration of biomolecule, which tend to rapidly occupy all the available reactive sites on the ZnO surface. This is more clear if we plot each capacitance normalized with respect to respective reagents value. In fact, in Figure 6 is more visible the higher capacitance increment of 150 nmol/ml concentration in comparison with 15 nmol/ml one.

The two tested concentrations are in the same range with other BSA sensors using a different transduction mechanism such as surface acoustic waves (60 nmol/ml)²⁹, gold nanospheres (~ 200 nmol/ml)³⁰, chemiluminescence (1.5 nmol/ml)³⁰ and cyclic voltammetry (~ 0.5 nmol/ml)³¹. The available reacting sites on the ZnO microwire surface, i.e. the estimated maximum density of amino-groups, was about 1.78 molecules/nm².

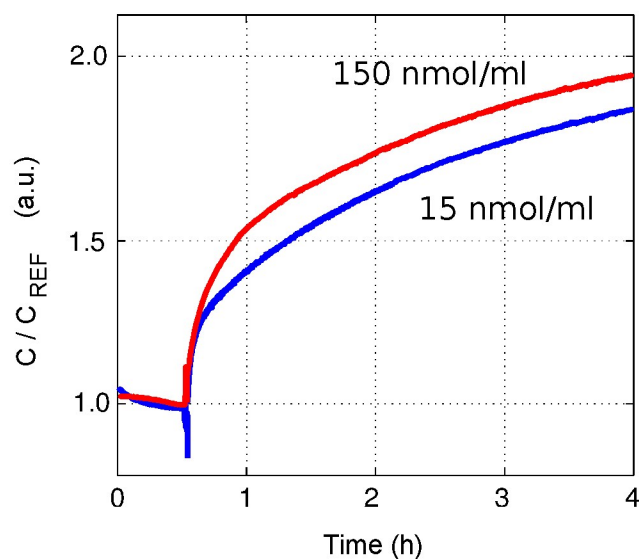


Fig. 6 ZnO normalized capacitances continuously measured during the EDC/Sulfo-NHS/BSA- NH_2 reaction. 150 nmol/ml concentration has an increase of about 100% over 4 hours. 15 nmol/ml concentration has an increase of about 75% over the same period of time.

After combining the ZnO- NH_2 microwires with the BSA protein in a concentration of 15 nmol/ml in a batch reaction, the amount of protein coupled to the ZnO- NH_2 surface, was 0.75 molecules/nm² (Supporting Information Figure S3). Thus, in absence of any other organic contamination one could assume this value as the maximum amount of proteins anchored to the $-\text{NH}_2$ groups of the ZnO surface. This is reasonable if compared to the number of available amino-reacting sites and considering the steric hindrance of the bulky BSA protein. This value can be considered the maximum final amount of conjugated protein that can be reached at the curve plateau of our real-time experiment.

4 Conclusions

We proposed an efficient and easy-to-use electronic platform which exploited a functionalized material integrated by dielectrophoresis onto gold-electrodes to measure in real-time a proof-of-concept proteins binding process. The DEP process and the real-time monitoring of protein binding onto the assembled ZnO- NH_2 microwire was carried out using a custom integrated electronic system directly connected to a PC for data storage. This can be considered the first step toward smart and portable integration of micro- and nanomaterials (e.g., microwires), electrodes and a CMOS chip for the detection of biomolecules. Moreover, such platform is suitable for multiparametric detection with different sensing materials. The platform is very sensitive thanks to the integration of the sensing chip and the readout circuit on the same PCB, and it can be easily combined with other commercial devices exploiting well-established Arduino ecosystem. Future works will concern parallel detection of different bio-probes by means of different functionalization or binding to increase the process selectivity and specificity.

Acknowledgement

The authors thank Dr. Laura Simone for her intensive work and professor M. Morelson for his support.

References

- 1 S. Krishnamoorthy, *Curr. Opin. Biotechnol.*, 2015, **34**, 118–124.
- 2 L. Lesser-Rojas, P. Ebbinghaus, G. Vasan, M.-L. Chu, A. Erbe and C.-F. Chou, *Nano Lett.*, 2014, **14**, 2242–2250.
- 3 S. Song, Y. Qin, Y. He, Q. Huang, C. Fan and H.-Y. Chen, *Chem. Soc. Rev.*, 2010, **39**, 4234–4243.
- 4 Y. Zhang, Y. Guo, Y. Xianyu, W. Chen, Y. Zhao and X. Jiang, *Adv. Mater.*, 2013, **25**, 3802–3819.
- 5 V. Cauda, P. Motto, D. Perrone, G. Piccinini and D. Demarchi, *Nanoscale Res. Lett.*, 2014, **9**, 1–10.
- 6 P. Motto, V. Cauda, S. Stassi, G. Canavese and D. Demarchi, *SENSORS*, 2013 IEEE, 2013, pp. 1–4.
- 7 D. Calestani, M. Zha, R. Mosca, A. Zappettini, M. Carotta, V. Di Natale and L. Zanotti, *Sens. Actuators, B*, 2010, **144**, 472–478.
- 8 A. Bonanno, M. Morello, M. Crepaldi, A. Sanginario, S. Benetto, V. Cauda, P. Civera and D. Demarchi, *IEEE Sensors J.*, 2015, **PP**, 1–1.
- 9 J. Suehiro, N. Nakagawa, S.-i. Hidaka, M. Ueda, K. Imasaka, M. Higashihata, T. Okada and M. Hara, *Nanotechnology*, 2006, **17**, 2567.
- 10 P. Nayak, B. Anbarasan and S. Ramaprabhu, *J. Phys. Chem. C*, 2013, **117**, 13202–13209.
- 11 T. Kavitha, A. I. Gopalan, K.-P. Lee and S.-Y. Park, *Carbon*, 2012, **50**, 2994–3000.
- 12 A. Menzel, K. Subannajui, F. Güder, D. Moser, O. Paul and M. Zacharias, *Adv. Funct. Mater.*, 2011, **21**, 4342–4348.
- 13 Y. Lei, X. Yan, N. Luo, Y. Song and Y. Zhang, *Colloids Surf., A*, 2010, **361**, 169–173.
- 14 Z. H. Ibupoto, N. Jamal, K. Khun and M. Willander, *Sens. Actuators, B*, 2012, **166**, 809–814.
- 15 M. Tak, V. Gupta and M. Tomar, *Biosens. Bioelectron.*, 2014, **59**, 200–207.
- 16 M. Tak, V. Gupta and M. Tomar, *Adv. Sci. Lett.*, 2014, **20**, 1337–1346.
- 17 S. K. Arya, S. Saha, J. E. Ramirez-Vick, V. Gupta, S. Bhansali and S. P. Singh, *Anal. Chim. Acta*, 2012, **737**, 1–21.
- 18 M. Laurenti, V. Cauda, R. Gazia, M. Fontana, V. F. Rivera, S. Bianco and G. Canavese, *Eur. J. Inorg. Chem.*, 2013, **2013**, 2520–2527.
- 19 V. F. Rivera, F. Auras, P. Motto, S. Stassi, G. Canavese, E. Celasco, T. Bein, B. Onida and V. Cauda, *Chem.–Eur. J.*, 2013, **19**, 14665–14674.
- 20 D. Wang, R. Zhu, Z. Zhou and X. Ye, *Appl. Phys. Lett.*, 2007, **90**, 103–110.
- 21 Y. Cui, Q. Wei, H. Park and C. M. Lieber, *Science*, 2001, **293**, 1289–1292.
- 22 A. Bonanno, M. Crepaldi, I. Rattalino, P. Motto, D. Demarchi and P. Civera, *IEEE Trans. Circuits Syst. I, Reg. Papers*, 2013, **60**, 975–988.
- 23 Arduino, <http://www.arduino.cc>, 2015.
- 24 G. T. Hermanson, *Bioconjugate Techniques*, Academic press, 2013.
- 25 F. Patolsky and C. M. Lieber, *Mater. Today*, 2005, **8**, 20–28.
- 26 A. J. Bard and L. R. Faulkner, *Electrochemical Methods: Fundamentals and Applications*, Wiley New York, 1980, vol. 2.
- 27 C. Argyo, V. Cauda, H. Engelke, J. Rädler, G. Bein and T. Bein, *Chem. Eur. J.*, 2012, **18**, 428–432.
- 28 A. Schloßbauer, A. M. Sauer, V. Cauda, A. Schmidt, H. Engelke, U. Rothbauer, K. Zolghadr, H. Leonhardt, C. Bräuchle and T. Bein, *Advanced Healthcare Materials*, 2012, **1**, 316–320.
- 29 K. Länge, G. Blaess, A. Voigt, R. Götzen and M. Rapp, *Biosens. Bioelectron.*, 2006, **22**, 227–232.
- 30 S. Dominguez-Medina, S. McDonough, P. Swanglap, C. F. Landes and S. Link, *Langmuir*, 2012, **28**, 9131–9139.
- 31 M.-W. Shao, H. Yao, M.-L. Zhang, N.-B. Wong, Y.-Y. Shan and S.-T. Lee, *Appl. Phys. Lett.*, 2005, **87**, 3106.

RSC Advances

